# Dipole and interfacial polarization phenomena in natural single-crystal calcite studied by the thermally stimulated depolarization currents method

N. Bogris*
*Solid Earth Physics Institute, University of Athens, Panepistimiopolis, Zografos 157 84, Athens, Greece*

J. Grammatikakis and A. N. Papathanassiou
*University of Athens, Physics Department, Solid State Physics Section, Panepistimiopolis, Zografos 157 84, Athens, Greece*
(Received 1 April 1998)

The low-temperature thermal depolarization spectrum of natural single-crystal calcite exhibits two relaxation mechanisms: the lower temperature (LT) one located at 188 K and the medium temperature (MT) one located at 230 K. Extensive thermally stimulated depolarization current (TSDC) experiments proved that the LT band is related to the rotation of defect dipoles, while the MT one to the interfacial polarization. A theoretical quantitative model, which involves the $SiO_2$ inclusions in the matrix, is developed and successfully interprets the appearance and the behavior of the MT band. [S0163-1829(98)02940-3]

## I. INTRODUCTION

The relaxation mechanisms that may exist in a dielectric are (i) the dipolar, (ii) the space charge, and (iii) the Maxwell-Wagner or interfacial polarization. The dipolar relaxation mechanisms,[1–8] result from dipoles created by the attraction of positive and negative charges existing in a dielectric. These charges can be created by doping the material with aliovalent impurities (i.e., in an alkali halide crystal $A^+B^-$, $M^{2+}$ impurities may substitute the $A^+$ cations). Due to the neutralization of the crystal, cation vacancies are created with negative effective charge. The impurity and the cation vacancies form a dipole known as $I$-$V$ dipole. Different kind of dipoles are created due to the distance between the impurity and the cation vacancy. When the impurity concentration is high, then dipole clusters may be formed, such as dimers, trimers, and so on.

Space charge relaxation,[9–11] is caused by both intrinsic and extrinsic free carriers (i.e., ions or electrons). The polarization of these charges is attributed to (i) the macroscopic movement of the charge carriers towards the electrodes and (ii) their accumulation at interfaces within the material. During the movement of the carriers, several processes may proceed simultaneously. Their parameters vary not only with time and space but they depend also on many variables atypical of the material.

Finally, the interfacial or Maxwell-Wagner (MW) relaxation mechanism,[9–11] usually appears in heterogeneous structures. It is the result of (i) the formation of charge layers at the interfaces, due to the different conductivity currents within the various phases, or (ii) the migration of the carriers over microscopic distances and the subsequent trapping. The materials that contain conductive inclusions are the most challenging materials for investigation.

In this paper the dielectric behavior of natural single calcite crystals is investigated, by applying the thermally stimulated depolarization currents (TSDC) method, in the temperature range from 77 to 400 K. We study the behavior of the peaks appearing in the spectrum by varying the initial experimental conditions, using different types of electrodes (conducting or insulating) and applying the partial heating technique. Finally we suggest an explanation for a part of the experimental results via a model that is more general than the well-known Maxwell-Wagner model.

## II. THEORY

### A. The method

The TSDC or ionic thermocurrents (ITC) method[12,13] is a high-resolution technique for electrical characterization of dielectrics. This method is as follows: The sample is polarized by an external applied electric field $E_p$, at a temperature $T_p$, for a duration time $t_p$ much longer than the relaxation time at the polarizing temperature, in order to orient the vast majority of the polarizing specimens existing in the sample. This polarization is subsequently frozen in by cooling (under the existence of the applied electric field) the sample to a temperature $T_0$ such that the frozen-in polarization remains unchanged even if the external electric field is switched off. This happens because at such a low temperature the relaxation time of the polarization processes is very big compared to that at room temperature. By heating up the sample by a constant heating rate $b$, the depolarization current, as the polarizing specimens relaxes, is detected by an electrometer. In the case of a single relaxation process obeying the usual Arrhenius relation,

$$\tau(T)=\tau_0\exp(E/kT), \tag{1}$$

where $\tau(T)$ is the relaxation time at the temperature $T$, $\tau_0$ is the preexponential factor, $E$ is the activation energy, and $k$ is the Boltzmann's constant, the depolarization current is given by the relation

$$i(T)=\frac{AP_0}{\tau_0}\exp\left(-\frac{E}{kT}\right)\exp\left\{\frac{1}{b\tau_0}\int_{T_0}^{T}e^{-(E/kT')}dT'\right\}, \tag{2}$$

 

where $A$ is the surface area of the sample and $P_0$ is the initial polarization. It is proven that the depolarization current is maximized at a temperature $T_m$ whenever the general condition[14]

$$\left[\frac{d\tau}{dt}\right]_{T=T_m} = -1 \tag{3}$$

is fulfilled. The above condition leads to the well-known equation for noninteracting dipoles:

$$T_m^2 = \frac{bE\tau_0}{k}\exp\left(\frac{E}{kT}\right). \tag{4}$$

For a single curve, the relaxation time $\tau(T)$ calculated according to the so-called area method is given by the formula[12,15]

$$\tau(T) = \frac{\int_{T_i}^{T_f} i(T)dT}{bi(T)}, \tag{5}$$

where $T_i$ is the temperature that the current appears and $T_f$ is the temperature that the current vanishes. An Arrhenius plot ($\ln\tau$ versus $T^{-1}$) permits the evaluation of $E$ and $\tau_0$.

The initial rise current for temperatures much smaller than the temperature $T_m$ (i.e., when $i_m \approx i_m/10$, where $i_m$ is the maximum current) is given by

$$i(T) = \frac{AP_0}{\tau_0}\exp\left(-\frac{E}{kT}\right). \tag{6}$$

From the logarithmic plot $\ln i(T)$ versus $T^{-1}$ the activation energy $E$ is directly derived.

The following characteristic features of the TSDC method make it especially suitable for investigating natural minerals, which are expected to include many defects. The method is very sensitive since it can measure dipole concentrations up to 0.1 ppm. The existence of a single peak in most cases is rather unrealistic even in ionic single crystals. Usually, many overlapping peaks may appear making the distinction and the calculation of the parameters very difficult. The TSDC method offers alternative experimental techniques in order to dissociate the different kinds of polarization mechanisms or to distinguish relaxation processes arising from polarization mechanisms with slightly different relaxation times. Finally the TSDC thermogram comprises several distinct mechanisms which in the conventional ac method would correspond to a frequency range from several GHz to a few mHz at room temperature.

### B. Maxwell-Wagner or interfacial depolarization

Several models of heterogeneous structures[16–18] (stratified structure, spherical or spheroid inclusions in the host matrix, etc.) have been adopted in order to explain the MW mechanism. The dielectric loss tangent and the relaxation time of the MW relaxation mechanism in a medium containing spheroid inclusions, as a function of (i) the electric permittivity, (ii) the conductivity of the inclusions and the host matrix, respectively, and (iii) the shape factor of the inclusions, are obtained. Provided that (i) all the inclusions are identical in shape and size, noninteracting and have their main axis parallel to the electric field and (ii) their conductivity is much higher than this of the host matrix, the relaxation time $\tau$ (for small volume fraction of the inclusions), is given by the relation[16–18]

$$\tau = \varepsilon_0\frac{(n_\alpha - 1)\varepsilon_1 + \varepsilon_2}{\sigma_2}, \tag{7}$$

where $\varepsilon_0$ is the electric permittivity of free space, $\varepsilon_1$ and $\varepsilon_2$ are the permittivities of the host matrix and the inclusions, respectively; $\sigma_2$ the conductivity of the inclusions and $n_\alpha$ the shape factor of the inclusions in a specific direction $\alpha$ (usually that of the applied electric field). When $\alpha = a$, $b$, or $c$ (where $a$, $b$, and $c$ are the axes of the spheroid inclusions, respectively) the shape factor is given by[18]

$$n_\alpha = \frac{2}{abcL_\alpha} \tag{8}$$

with

$$L_\alpha = \int_0^\infty \frac{d\lambda}{(\alpha+\lambda)^2\sqrt{(a^2+\lambda)(b^2+\lambda)(c^2+\lambda)}}.$$

The small volume fraction approximation is generally fulfilled in materials that are studied using the TSDC method. The condition $\sigma_1 \ll \sigma_2$ (in some cases it is assumed $\sigma_1 = 0$) is also important since with the TSDC method we can study only insulating materials. When the conductivity inside the inclusion particles is thermally activated, i.e.,

$$\sigma_2 = \sigma_0\exp(E/kT), \tag{9}$$

where $\sigma_0$ is a preexponential factor, $E$ is the activation energy, and $k$ is the Boltzmann's constant, then the relaxation time is found to be an exponential function of the temperature as in an Arrhenius-type relation:

$$\tau(T) = \tau_0\exp(E/kT)$$

with

$$\tau_0 = \varepsilon_0\frac{(n_\alpha - 1)\varepsilon_1 + \varepsilon_2}{\sigma_0}. \tag{10}$$

For a first-order kinetic process, the equations of the TSDC method are the same as in the previous section.

### C. Calcite structure

The unit cell in calcite's structure[19] is an exact rombohedron, which contains two molecules of $CaCO_3$. The hexagonal cell (when using an hexagonal axis system) is of the same height of the exact rombohedron but contains six molecules of $CaCO_3$. By looking at the crystalline structure of natural calcite along the $c$ axis, it is observed that groups of calcite basis $CO_3^{2-}$ that belong to the same layer are of the same orientation, while those that belong to adjacent layers are of different orientation.

## III. EXPERIMENTAL DETAILS

Natural calcite single crystals were used for TSDC experiments. Atomic absorption spectroscopy (AAS) indicates the

TABLE I. Impurity concentrations existing in natural calcite single crystals.

| Impurity | Concentration (ppm) |
|---|---|
| $Na^+$ | 579 |
| $K^+$ | 125 |
| $Mn^{2+}$ | 211 |
| $Mg^{2+}$ | 745 |
| $Sr^{2+}$ | 229 |
| Fe | 125 |
| $Al^{3+}$ | <200 |
| **$Si^{4+}$** | **4995** |
| $Ti^{4+}$ | 586 |

presence of impurities with concentrations presented in Table I. Note that $Si^{4+}$ has the greatest concentration of all the impurities. This impurity is found in inclusions of $SiO_2$ in calcite crystals.[26] This coincides with the fact that in other samples of polycrystal calcite[20] inclusions of $SiO_2$ were observed.

The specimens were cut along the cleavage planes of calcite. Their thickness was 1.0–1.5 mm and care was taken to avoid contamination with moisture. The samples were placed onto platinum electrodes in a cryostat operated from liquid nitrogen temperature (LNT) up to 450 K. A vacuum of $10^{-4}$ Torr was created. The temperature was measured via a thermocouple connected to an Air Products temperature controller. The temperature variation was monitored by the controller and the desired (constant) heating rate was maintained throughout each TSDC scan. The crystals were polarized by using a Keithley 700-A dc power supply. The depolarization current was measured via a Carry 401 electrometer. The signals from the temperature controller and the electrometer were digitized via an $A/D$ card installed into a personal computer. The experimental data were processed by using computer analysis software.

## IV. EXPERIMENTAL RESULTS

### A. As received samples

We performed TSDC measurements on as grown natural calcite crystals in the temperature range from LNT up to 400 K. The external polarization electric field intensity was usually less than 20 kV/cm, while the heating rate was kept constant and equal to 4 K/min, or less.

A typical thermogram of an as grown crystal is shown in Fig. 1. Three bands were detected: the lower-temperature (LT) band at a temperature $T_m$ (where the current reaches a maximum) equal to 188 K, the medium-temperature (MT) band with maximum around 230 K and the high-temperature (HT) band with maximum above room temperature (near 320 K). We focused on the study of the lower-temperature bands (MT and LT).

### B. Results from the MT band

#### *1. Dependence on the electrode material*

Figure 2 shows the MT band when platinum [metal-sample-metal (MSM) structure], or insulating electrodes [metal-insulator-sample-insulator-metal (MISIM)], are used. The other experimental conditions were kept constant. An inspection of Fig. 2 results in the fact that the MT band is practically insensitive to the electrode material indicating the existence of a bulk phenomenon.

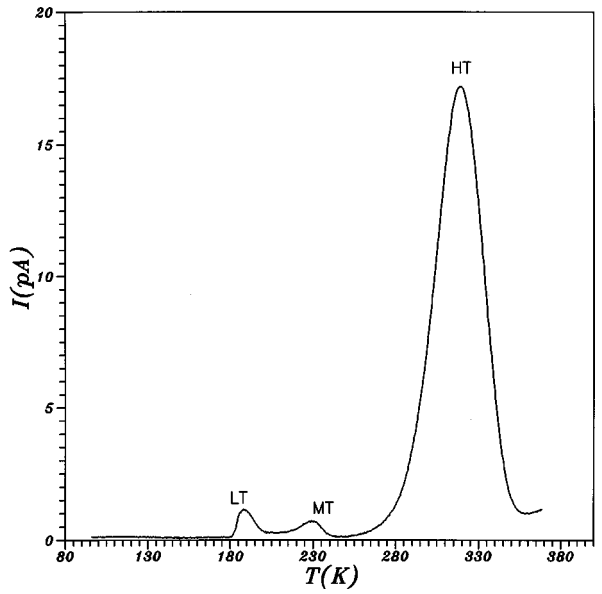


FIG. 1. TSDC scan of as grown natural calcite single crystal. The external polarization electric field is $E_p = 19.6$ kV/cm, the polarizing temperature $T_p = 288$ K, the polarizing duration time $t_p = 5$ min and the heating rate $b = 3.8$ K/min.

#### *2. Reproducibility of the MT band*

In Fig. 3 we depict a series of successive TSDC scans obtained under exactly the same experimental conditions. A shift of the peak towards higher temperatures and a simultaneous decrease of the height of the peak are observed. The same happens when insulating electrodes are used. The total

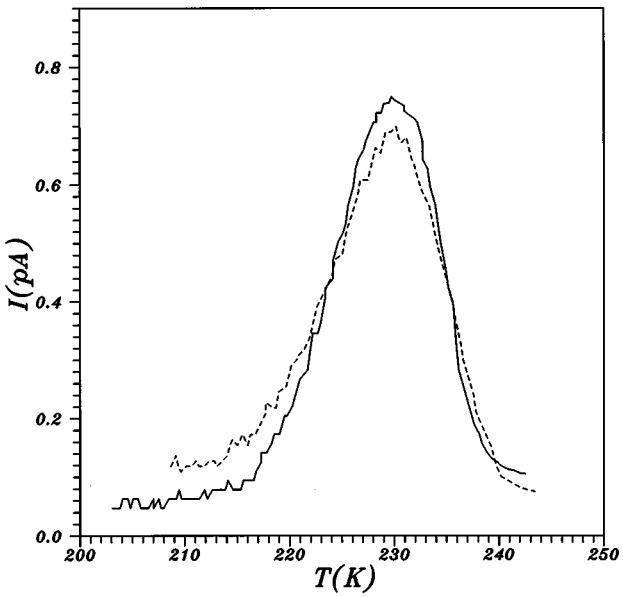


FIG. 2. TSDC scans of MT band of natural calcite single crystal with platinum electrodes (solid line) and insulating electrodes (dashed line).

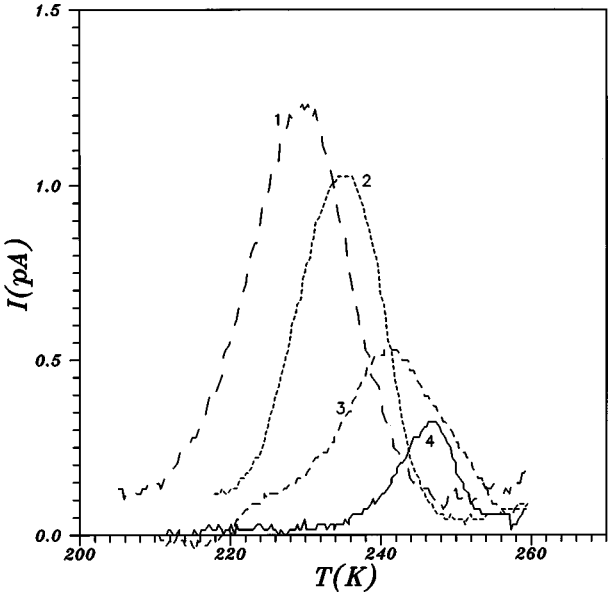


FIG. 3. A series of successive TSDC scans of MT band under exactly the same experimental conditions. 1, first TSDC scan; 2, second TSDC scan; 3, third TSDC scan; 4, fourth TSDC scan.

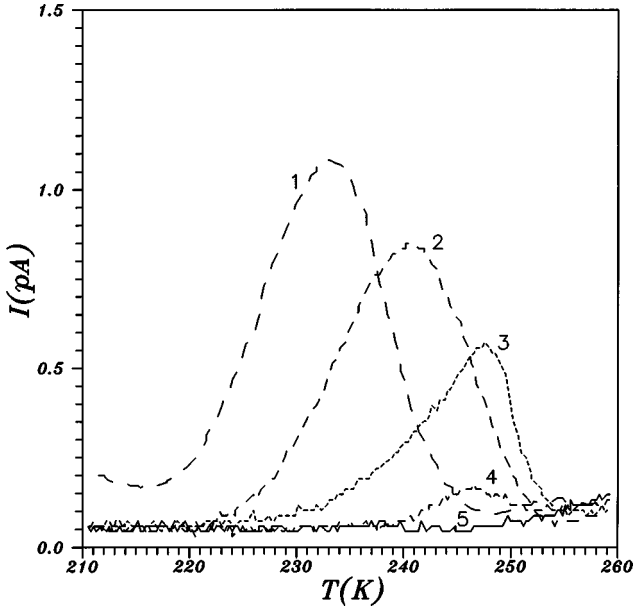


FIG. 4. A series of successive TSDC scans of MT band after thermal annealing under exactly the same experimental conditions. 1, first TSDC scan; 2, second TSDC scan; 3, third TSDC scan; 4, fourth TSDC scan; 5, fifth scan.

charge released, which is proportional to the area under the peak and is a measure of the concentration of the carriers that contribute to the relaxation process, is also a decreasing function of the successive scans.

All the results of our samples, indicate that, in the first TSDC scan, the maximum of the band arises at around 230 K, in the second at around 235 K, in the third at around 241 K and in the fourth at around 248 K. This behavior is observed when the sample has relaxed for a long time compared to the time needed to perform the set of the successive TSDC scans. Furthermore, in some of the samples, during the fourth or fifth scan the signal was so weak that it was hardly detected or it was masked by the intense HT band. The variation of the experimental conditions (i.e., the external electric-field density $E_p$, the polarization time $t_p$, and polarization temperature $T_p$), did not give any information due to the irreproducibility of the spectra.

### *3. Thermal treatment of the MT band*

In order to gain more information concerning the origin of the peak, and specially to evaluate the contribution of dipoles on this one, we thermally perturbed the samples and immediately afterwards the samples were frozen. If the peak results from a dipolar relaxation mechanism, the thermal treatment decomposes the agglomerates and liberates $I$-$V$ dipoles and consequently the size of the resultant TSDC peak is maximized. Therefore, we annealed the samples at the temperature range from 600 to 800 K for a time interval of 30 min or less and then we quenched the samples to RT. We did not anneal the samples at higher temperatures in order to avoid the chemical decomposition of the sample.

Figure 4 depicts a series of successive TSDC scans just after the thermal treatment of the sample. The annealing temperature was 700 K and the annealing time 30 min. No significant difference was observed in comparison to the untreated samples; neither the position nor the amplitude of the peak was changed. The same results were obtained when the samples were annealed at different temperatures for different periods of time.

### *4. Activation parameters of the MT band*

The shape of the MT peak recorded using either platinum or teflon electrodes, is rather symmetrical (see Fig. 2), indicating that more than one relaxation mechanism contributes to the peak. An $\ln \tau$ versus $1/T$ plot is shown in Fig. 5. A main relaxation peak is observed together with a small contribution of another one at the low-temperature side. The curvature of the $\ln \tau$ versus $1/T$ plot is probably caused by the overlap of the LT and MT bands, but this assumption fails if we try to analyze the other peaks appearing in the

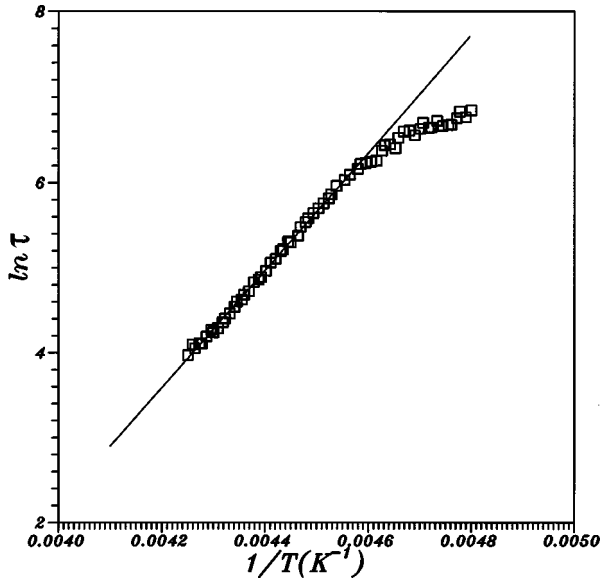


FIG. 5. An $\ln \tau$ vs $1/T$ Arrhenius plot for the MT band with maximum at $T_m = 230$ K.

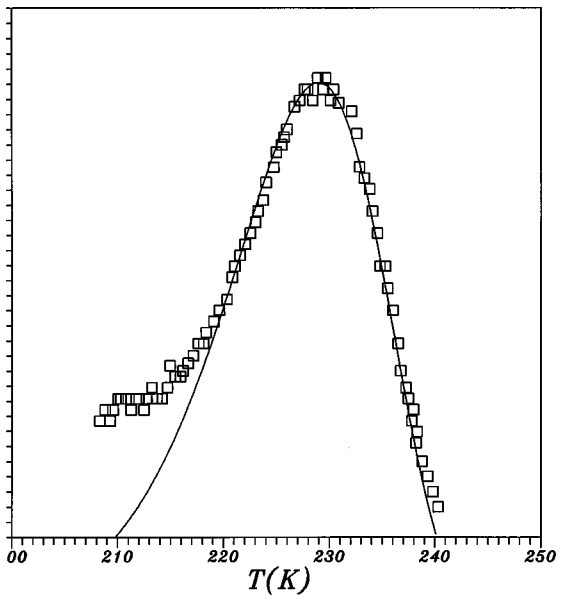


FIG. 6. The fit (solid line) to the experimental data (squares) of MT band.

successive TSDC scans, when there is no overlapping (see Fig. 3). On the other hand the $\ln \tau$ versus $1/T$ plots indicate that there does remain a small contribution of another mechanism (see also Fig. 6 where a fit to the experimental data is shown). Due to these facts, we calculated only the activation parameters (the activation energy $E$ and the preexponential factor time $\tau_0$), for the high-temperature mechanism (see Table II). The dependence of the activation energy upon the temperature $T_m$, where the current reaches its maximum, is shown in Fig. 7. An increase of the activation energy as the temperature increases is observed.

### C. Results from the LT band

We proceeded to the study of the LT band in a manner similar to that followed for the MT band. The use of different types of electrodes (see Fig. 8) revealed that there is no significant change in the amplitude and the position of the peak, thus indicating bulk polarization. Successive TSDC scans under exactly the same experimental conditions, depict a decrease of the intensity of the peak while $T_m$ remains almost the same (see Fig. 9). After the annealing of the samples (performed in the same way as for the MT band), no significant change was observed. Only a small shift in $T_m$ towards higher temperatures (4–5 K) is observed. The $\ln \tau$ versus $1/T$ plot indicates that two relaxation mechanisms contribute to the LT band (see Fig. 10); the activation parameters (i.e., the activation energy $E$ and the preexponential factor $\tau_0$) are presented in Table III.

TABLE II. Activation parameters of the MT band calculated from a series of successive TSDC scans.

| $T_m$ (K) | $E$ (eV) | $\tau_0$ (sec) |
|---|---|---|
| 230 | $0.59 \pm 0.02$ | $9.63 \times 10^{-12}$ |
| 235 | $0.73 \pm 0.03$ | $2.54 \times 10^{-14}$ |
| 240 | $0.69 \pm 0.03$ | $2.93 \times 10^{-13}$ |
| 242 | $0.71 \pm 0.03$ | $2.72 \times 10^{-13}$ |
| 249 | $0.81 \pm 0.03$ | $4.18 \times 10^{-15}$ |

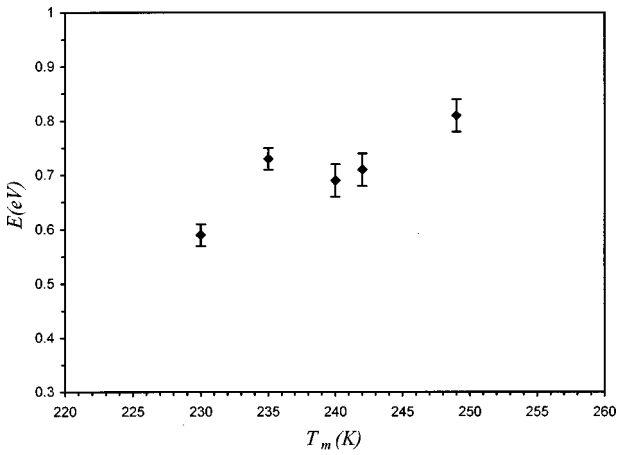


FIG. 7. The dependence of activation energy on the temperature $T_m$ for the MT band.

## V. DISCUSSION

### A. Attribution of the MT band: A step beyond the MW model

We summarize the features of the MT band as follows. (i) Its position and its height does not change even if we use different electrode configurations (MSM or MISIM). (ii) Successive TSDC scans result in a shift to higher temperatures and simultaneously in a progressive decrease of the height of the observed peaks. (iii) The thermal treatment does not affect the above process. (iv) The activation energy increases as the temperature increases.

Due to the first feature it is concluded that the MT band is not the result of surface polarization (space-charge relaxation) but it is a bulk phenomenon. The rest of the features indicate that this band is not the result of the contribution of a simple dipolar relaxation mechanism, since the shift of the

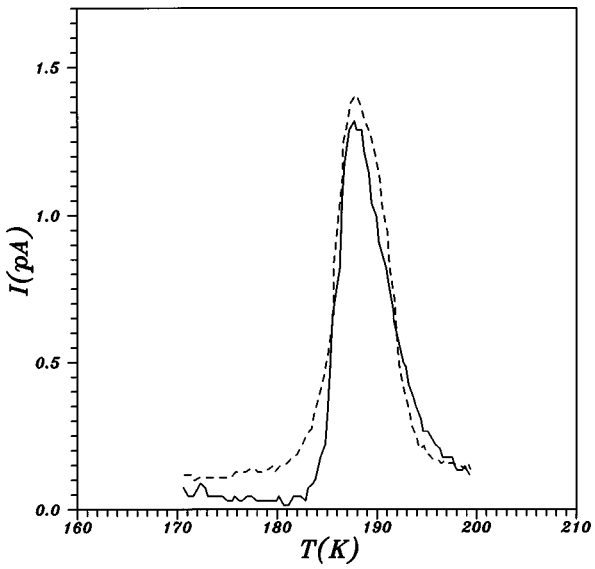


FIG. 8. TSDC scans of LT band of natural calcite single crystal with platinum electrodes (solid line) and insulating electrodes (dashed line).

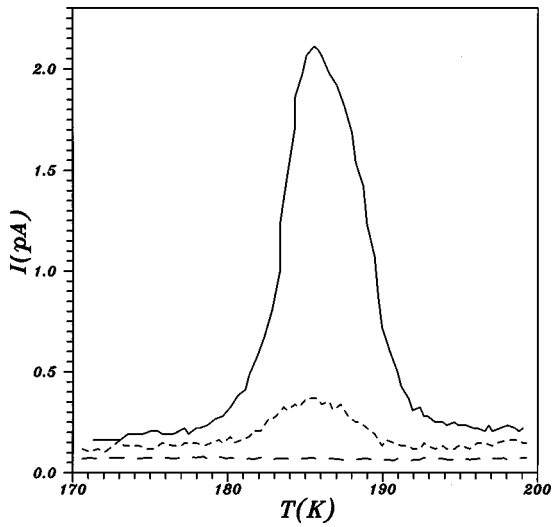


FIG. 9. A series of successive TSDC scans of LT band under exactly the same experimental conditions. Solid line, first scan; dotted line, second scan; dashed line, third scan.

peak in a set of successive scans is not a characteristic of dipole peaks. Indeed, (i) by assuming the probable formation of clusters, which leads to the decrease of the single dipoles population, the continuous shift of the peak to higher temperatures cannot be explained and (ii) by accepting the presence of a complicated dipolar relaxation mechanism with distribution in relaxation time, the shift of the peak to higher temperatures and the simultaneous decrease of its height are not justified, as the polarization temperature is always above the region that the MT band is appeared.

It is suggested[22–25] that the irreproducibility of the MT band may be caused by the intense HT band, which is probably related to space-charge polarization. In this paper we show that the MT band should be attributed to interfacial polarization and we present a quantitative model (based on the interfacial polarization), which fits very well to the experimental data.

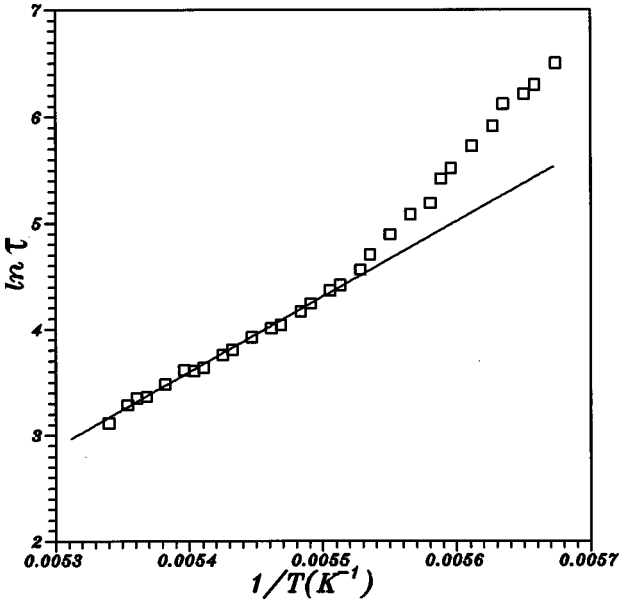


FIG. 10. An $\ln \tau$ vs $1/T$ Arrhenius plot for the LT band.

TABLE III. Activation parameters of the low- and high-temperature relaxation mechanism in the LT band.

| $T$ (K) | $E$ (eV) | $\tau_0$ (sec) |
|---|---|---|
| 180–185 | $0.35 \pm 0.02$ | $3.90 \times 10^{-8}$ |
| 187–193 | $0.65 \pm 0.02$ | $1.33 \times 10^{-16}$ |

The $SiO_2$ found in our specimens can be in the form of inclusions in the host matrix or can be distributed between the cleavage planes of calcite.[26] According to the MW model (see Sec. II B), for the small volume fraction and for the case where the conductivity of the inclusions is much higher than that of the host matrix, the relaxation time $\tau$ is given by the relation

$$\tau = \varepsilon_0 \frac{(n_\alpha - 1)\varepsilon_1 + \varepsilon_2}{\sigma_2},$$

where $\varepsilon_0$ is the permittivity of free space; $\varepsilon_1$ and $\varepsilon_2$ are the permittivity of the calcite and the $SiO_2$, respectively; $\sigma_2$ is the conductivity of the $SiO_2$; and $n_\alpha$ the shape factor. By substituting to the above relation the parameters[21] $\varepsilon_1 \cong 8$, $\varepsilon_2 \cong 4.5$, and $\sigma_2 = 3 \times 10^{-11}$ $(\Omega \mathrm{m})^{-1}$ [notice that the conductivity of calcite is $\sigma_1 = 2 \times 10^{-13}$ $(\Omega \mathrm{m})^{-1}$] and taking $n_\alpha = 1$, it is derived that the relaxation time at room temperature is approximately 0.6 sec. Even using the exact relation where it is not assumed that the conductivity of the inclusions is much more higher than that of the host matrix, the difference in the above calculation is negligible. By substituting the activation parameters of the MT band that were derived from our experimental analysis (see Table II) into the Arrhenius relation, it is deduced that the relaxation time of the MT band at room temperature varies from 0.1 up to 0.01 sec. The comparison between the theoretical and experimental relaxation times, indicates that the MT band is probably attributed to MW polarization.

Furthermore, we shall prove that when the population $N$ of the carriers (trapped in the interfaces between the inclusions and the host matrix and contributing to MW polarization) varies, we theoretically expect a shift of the TSDC peak to higher temperatures with simultaneous variation of its height.

The MW model (presented in Sec. II B) assumes the ideal case of conductive inclusions ($\sigma \to \infty$) in a perfect insulator ($\sigma = 0$) and thus the full trapping of the carriers in the interfaces is expected; but when this condition is not generally fulfilled, the full trapping of the carriers in the interfaces does not happen. When the conductivity of the inclusions is described by an exponential behavior, then the relaxation time has the form of the Arrhenius relation,

$$\tau(T) = \tau_0 \exp(E/kT),$$

where

$$\tau_0 = \varepsilon_0 \frac{(n_\alpha - 1)\varepsilon_1 + \varepsilon_2}{\sigma_0}.$$

The quantity $\sigma_0$ is proportional to the population $N$ of the carriers. The decrease of the population leads also to the decrease of the height of the peak and to the increase of the

preexponential factor $\tau_0$ (since $\sigma_0$ also decreases). The increase of $\tau_0$ results in the shift of the peak to higher temperatures [according to Eq. (4)]. It is also easily shown that this shift results when the activation energy increases.

By summarizing, we conclude to the following (assuming that the carriers are not fully trapped): (i) even if the carriers are of the same type (i.e., they do not interact) and even if the inclusions have exactly the same geometry, a shift of the peak with simultaneous variation of its height is expected, when the population of the carriers varies and (ii) the shift of the peak also takes place when a variation in the activation energy occurs.

From Table II, where the calculated values of the activation energy $E$ and the preexponential factor $\tau_0$ of MT band are given, the increase of the activation energy is experimentally confirmed, thus indicating the shift of the peak to higher temperatures. Furthermore, as the difference between the conductivity of the host (calcite) and the inclusions ($SiO_2$) is not so big, the carriers in the inclusions may not be fully trapped, resulting in the decrease of the MT band under successive scans. The expected (within the model) theoretical increase of the preexponential factor (when the height of the peak decreases) is not clear, because of the usually large errors appearing in the calculation of that factor.

Finally, a basic difference between a single dipolar and an interfacial polarization relaxation mechanism can be asserted: The decrease of the population of dipoles for several reasons (i.e., clustering) does not lead to the shift of the peak, but only to the decrease of its height; on the other hand, variation of the population $N$ in the interfacial polarization leads to the variation of the position and height of the peak.

### B. Attribution of the LT band

We summarize the features of the LT band as follows. (i) The LT peak does not depend on the different electrode configuration. (ii) Under successive scans, the height of the peak decreases, but $T_m$ remains practically unchanged. (ii) The thermal anneal does not drastically affect the features of the peak. The above characteristics support a dipolar relaxation mechanism. The small variations in the height and in the position of the peak after the thermal treatment possibly originate from the variation of the population of the dipoles that contribute to the peak.

## VI. CONCLUSIONS

By using the TSDC method we studied the relaxation mechanisms existing in single crystal-calcite samples. The analysis of the MT band indicates that a MW relaxation mechanism contributes to that peak. This mechanism is theoretically predicted, and seems to be experimentally confirmed. By extending the well-known MW model, the characteristics of that peak are explained. The activation energy of that peak was found to vary from 0.59 eV to 0.83 eV. The analysis of the LT band indicates that two dipolar relaxation mechanisms contribute to that peak with activation energies 0.35 eV and 0.65 eV, respectively.

## ACKNOWLEDGMENT

The authors would like to thank Professor P. Pissis from the National Technical University of Athens for fruitful discussions.

*Electronic address: nbogris@atlas.uoa.gr

[1] J. Grammatikakis, C. A. Londos, V. A. Katsika, and N. Bogris, J. Phys. Chem. Solids **50**, 845 (1989).
[2] V. Katsika, J. Grammatikakis, N. Bogris, A. Kyritsis, and A. Papathanassiou, Phys. Rev. B **44**, 12 686 (1991).
[3] J. Grammatikakis, A. Papathanassiou, N. Bogris, M. Manolopoulos, and V. Katsika, Phys. Rev. B **46**, 12 146 (1992).
[4] M. Suszynska and R. Capelleti, Acta Phys. Pol. **80**, 129 (1991).
[5] C. H. Burton and J. S. Dryden, J. Phys. C **3**, 523 (1970).
[6] C. A. Londos, N. Gouskos, J. Grammatikakis, N. Bogris, A. Kyritsis, and A. Papathanassiou, J. Phys. Chem. Solids **53**, 249 (1992).
[7] J. P. Stott and H. Crawford, Jr., Phys. Rev. B **4**, 668 (1971).
[8] E. L. Kitts, Jr. and J. H. Grawford, Jr., Phys. Rev. B **4**, 5264 (1974).
[9] J. van Turnhout, *Thermally Stimulated Discharge of Polymer Electrets* (Elsevier Scientific, New York, 1975).
[10] R. G. Multhaupt, B. Gross, and G. M. Sessler, in *Recent Progress in Electret Research,* edited by G. M. Sessler Electrets, 2nd ed. (Springer-Verlag, Berlin, 1987).
[11] R. G. Multhaupt, IEEE Trans. Electr. Insul. **EI-22**, 5 531 (1987).
[12] C. Bucci and R. Fieschi, Phys. Rev. Lett. **12**, 16 (1964).
[13] C. Bucci and R. Fieschi, Phys. Rev. **148**, 816 (1966).
[14] P. Varotsos, N. G. Bogris, and A. Kyritsis, J. Phys. Chem. Solids **53**, 1007 (1992).
[15] S. Radhakrishna and S. Haridoss, Cryst. Lattice Defects **7**, 191 (1978).
[16] T. Hanai, *Emulsion Science,* edited by P. Sherman (Academic, London, 1968), Chap. 5.
[17] L. H. Van Beek, in *Dielectric Relaxation of Heterogeneous Systems,* edited by J. B. Birks, Progress in Dielectrics (Heywood, London, 1967), Vol. 7.
[18] R. Villa and M. J. de Castro, J. Phys. D **25**, 1357 (1992).
[19] R. J. Reeder, *Carbonates: Mineralogy and Chemistry in Reviews in Mineralogy* (Mineralogical Society of America, Washington, D.C., 1983), Vol. 11.
[20] N. Bogris, Ph.D. thesis, University of Athens, 1994.
[21] M. Beblo, A. Berktold, V. Bleil, H. Gebrande, B. Grauert, U. Haak, V. Haak, H. Kern, H. Miller, N. Petersen, J. Pohl, F. Rummel, and J. R. Schopper, in *Physical Properties of Rocks,* Lanndölt Bornstein New Series, Group V, Vol. 1, Pt. b (Springer-Verlag, Berlin, 1982).
[22] A. Papathanassiou and J. Grammatikakis, Phys. Rev. B **53**, 16 252 (1996).
[23] A. Papathanassiou and J. Grammatikakis, Phys. Rev. B **56**, 8590 (1997).
[24] A. Papathanassiou and J. Grammatikakis, J. Phys. Chem. Solids **58**, 1063 (1997).
[25] A. Papathanassiou *et al.*, Radiat. Eff. Defects Solids **134**, 247 (1995).
[26] Dr. Katerinopoulos and Dr. Magganas (personal communication).